Mutant Sodium Channel for Tumor Therapy

Bakhos A Tannous[1–3], Adam P Christensen[3,4], Lisa Pike[1], Thomas Wurdinger[1–3], Katherine F Perry[1], Okay Saydam[1,3], Andreas H Jacobs[5], Jaime García-Añoveros[6], Ralph Weissleder[2,7,8], Miguel Sena-Esteves[1], David P Corey[3,4,9] and Xandra O Breakefield[1–3]

[1]Department of Neurology, Molecular Neurogenetics Unit, Massachusetts General Hospital, Harvard Medical School, Boston, Massachusetts, USA; [2]Department of Radiology, Center for Molecular Imaging Research, Massachusetts General Hospital, Harvard Medical School, Boston, Massachusetts, USA; [3]Program in Neuroscience, Harvard Medical School, Boston, Massachusetts, USA; [4]Department of Neurobiology, Harvard Medical School, Boston, Massachusetts, USA; [5]Laboratory for Gene Therapy and Molecular Imaging at the MPI for Neurological Research, Cologne, Germany; [6]Department of Anesthesiology, Northwestern University Feinberg School of Medicine, Chicago, Illinois, USA; [7]Center for Systems Biology, Massachusetts General Hospital, Harvard Medical School, Boston, Massachusetts, USA; [8]Department of Systems Biology, Harvard Medical School, Boston, Massachusetts, USA; [9]Howard Hughes Medical Institute, Chevy Chase, Maryland, USA

Viral vectors have been used to deliver a wide range of therapeutic genes to tumors. In this study, a novel tumor therapy was achieved by the delivery of a mammalian brain sodium channel, ASIC2a, carrying a mutation that renders it constitutively open. This channel was delivered to tumor cells using a herpes simplex virus-1/Epstein–Barr virus (HSV/EBV) hybrid amplicon vector in which gene expression was controlled by a tetracycline regulatory system (tet-on) with silencer elements. Upon infection and doxycycline induction of mutant channel expression in tumor cells, the open channel led to amiloride-sensitive sodium influx as assessed by patch clamp recording and sodium imaging in culture. Within hours, tumor cells swelled and died. In addition to cells expressing the mutant channel, adjacent, noninfected cells connected by gap junctions also died. Intratumoral injection of HSV/EBV amplicon vector encoding the mutant sodium channel and systemic administration of doxycycline led to regression of subcutaneous tumors in nude mice as assessed by *in vivo* bioluminescence imaging. The advantage of this direct mode of tumor therapy is that all types of tumor cells become susceptible and death is rapid with no time for the tumor cells to become resistant.

Received 13 May 2008; accepted 31 January 2009; published online 3 March 2009. doi:10.1038/mt.2009.33

INTRODUCTION

Delivery of therapeutic genes to tumors through viral vectors offers an exciting approach to augmentation of cancer therapies.[1–3] A number of therapeutic genes have shown to have potential in experimental models, including genes encoding immune-enhancing functions,[4,5] prodrug activation enzymes,[6,7] and apoptotic proteins.[8] Other strategies have targeted channels on tumor cells, including the sodium iodide symporter, which can increase influx of ^{125}I for tumor killing and ^{123}I for imaging,[9] and chloride channels—with ^{201}Tl-choride and ^{131}ITM-601 used for therapy and imaging, respectively.[10,11] An increasing number of studies have shown that gene therapy strategies can be additive or synergistic with each other and with ongoing neurosurgical, chemical, and radiation therapies. Given that only a small percentage of cells in the tumor mass express the transgene following vector delivery, usually ~1–5% after direct intratumoral injection,[12] it is essential that the transgene product have a "bystander" effect, such that adjacent, uninfected tumor cells are also killed. In parallel, it is also important to maximize gene delivery to tumor cells, which has been achieved for human gliomas with intratumoral injection of oncolytic viruses,[13] convection-enhanced delivery of nonreplicating vectors,[14] and modification of the extracellular matrix.[15] Amplicon vectors derived from herpes simplex virus type 1 (HSV-1) have been used both for direct intratumoral delivery of therapeutic genes,[16] as a platform for generation of retrovirus vectors,[17] and for maintenance of transgenes either by episomal replication using Epstein–Barr virus (EBV) elements[18] or by genomic integration using adeno-associated virus elements.[19]

The ASIC2 ion channel (previously known as BNC1, BNaC1, or MDEG) is a member of the DEG/ENaC superfamily of ion channel subunits.[20] Members of this family have two membrane-spanning domains with a large extracellular loop and can assemble in a homomeric or heteromeric configuration with three subunits in a channel.[21] They are mostly selective for Na^+, and they are normally activated by low pH. Specific mutations (G430 to T, V, or F) in the second transmembrane domain of ASIC2 cause the channel to be constitutively active, conducting Na^+ even at physiological pH. The glycine at position 430 or its equivalent is perfectly conserved among the ASIC family. Crystal structure of ASIC1 predicts that G430 in ASIC2 is located in the second transmembrane domain, at an interface with the first transmembrane domain of the adjacent subunit and near a kink-forming glycine that may be involved in gating.[21] *Xenopus* oocytes and HEK293 cells expressing mutant ASIC2 swell and die.[22] The homologous mutation (A692V) in another DEG/ENaC channel, the nematode UNC-105, causes the channel to be hyperactive, generating a constitutive Na^+ influx that depolarizes the cells and kills them.[23] Similarly, the homologous mutations in the related ion channels

Correspondence: *Bakhos A Tannous, Department of Neurology, Molecular Neurogenetics Unit, Massachusetts General Hospital-East, Building 149, 13th Street, Charlestown, Boston, Massachusetts, 02129 USA. E-mail: btannous@hms.harvard.edu*

in nematodes, MEC-4 and DEG-1, cause neuronal degeneration presumably by the same mechanism.[24,25] Most of these gain-of-function mutations are dominant, in the sense that a mutation in just one subunit of a trimeric channel can unblock the channel pore, leading to constitutive Na^+ influx and cell death.[25]

At this instance, we describe, for the first time, the use of a mutant form of the human brain sodium channel ASIC2 for tumor therapy. There are two splice forms of human ASIC2, a and b. In these studies we used ASIC2a in which the conserved G at position 430 was mutated to F (G430F).[22] Mutant or wild-type sodium channel cDNAs were cloned into an HSV/EBV hybrid amplicon vector in which control of the channel and red fluorescent protein (RFP) expression is under a bidirectional tetracycline regulated (tet-on) promoter and control of enhanced green fluorescent protein (eGFP) is under an immediate early (IE) HSV promoter.[26,27] In this configuration the level of induction (RFP) and the extent of gene delivery (eGFP) can both be visualized. When tumor cells were infected with the vector encoding the mutant channel and exposed to dox, they died within 12 hours, while they remained viable in the absence of tet or when the vector encoded the wild-type channel. Importantly, the toxic effect of this mutant-channel killing mechanism—likely mediated by ion influx—was shown to spread from infected cells to adjacent noninfected cells via gap junctions, as visualized microscopically by flow of fluorescent dyes between cells and as measured by bioluminescence. This killing mechanism was shown to be effective for tumor regression *in vivo* in a xenograft model by intratumoral injection of mutant sodium channel vectors and systemic delivery of dox.

RESULTS

Tet-on inducible hybrid vector

We used a HSV/EBV hybrid amplicon construct consisting of: an HSV amplicon backbone containing the EBV origin of replication (oriP) and a mutant *EBNA-1* gene to mediate episomal replication of amplicon sequences in synchrony with replication of genomic DNA in the host cell nucleus;[18] expression cassettes encoding the tet-silencer and activator proteins[27] under the cytomegalovirus IE promoter to regulate transgene expression through the inducible promoter; and eGFP under the HSV-1 IE4/5 promoter to monitor transduction efficiency.[26] This construct also contains a bidirectional tet-responsive promoter,[28] driving the expression of RFP and either the wild-type ($ASIC2^{wt}$) or the mutant ($ASIC2^{G430F}$) human brain ASIC2 sodium channel, with corresponding amplicons termed, $pHET14B\text{-}ASIC2^{wt}$ and $pHET14B\text{-}ASIC2^{G430F}$, respectively (**Figure 1a**, generically termed HET14B-ASCIC2). HSV/EBV hybrid amplicon vectors were packaged using the helper-virus-free system, as described,[29] in the absence of dox. Upon viral transduction, eGFP was expressed; then when cells

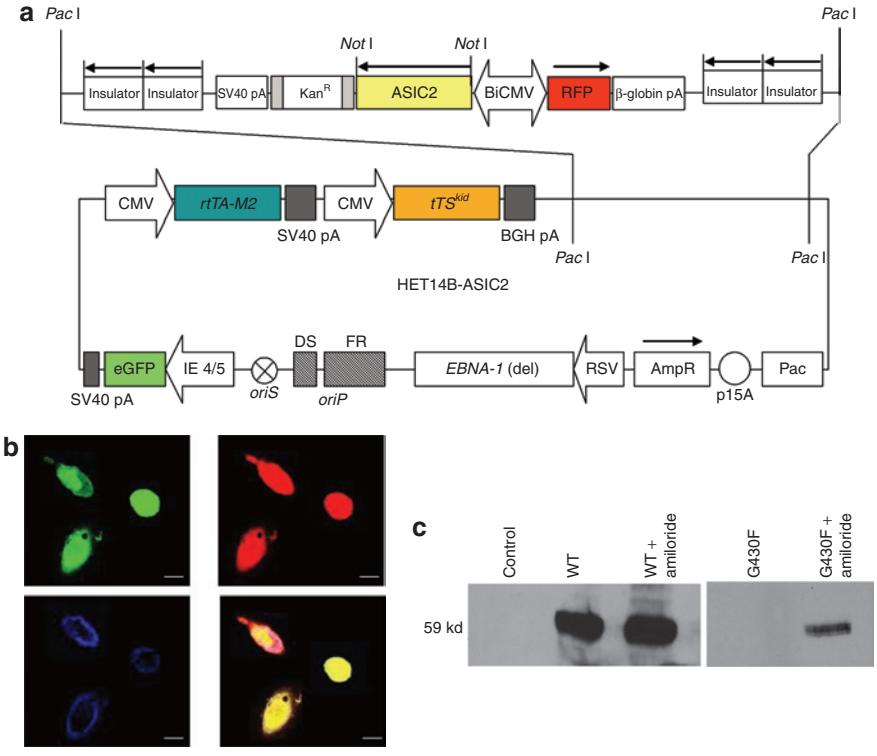

Figure 1 Cloning and expression of the mutant and wild-type sodium channel in HSV/EBV hybrid vector. (**a**) cDNAs for the mutant (G430F) and the wild-type ASIC2a sodium channels were cloned into the HSV/EBV hybrid amplicon, pHET14B under the control of a bidirectional tet responsive promoter. Components of the amplicon are described in Methods. (**b,c**) CHO cells were transduced with $pHET14B\text{-}ASIC2^{wt}$ or $pHET14B\text{-}ASIC2^{G430F}$ in the presence of dox with or without amiloride. (**b**) Viable cells expressing the wild-type channel were replated on coverslips, fixed, and immunostained for the ASIC2 channel. Green fluorescence shows that the infected cells are expressing eGFP (top left); red fluorescence signals that the transgene is turned on by doxy (top right); blue represents the ASIC2 immunostaining (bottom left). An overlay of all images is also shown (bottom right). Bar = 20 μm. (**c**) Cells were lysed 16 hours post-transfection and proteins (100 μg/sample) were analyzed by SDS-PAGE and western blotting using the ASIC2 antibodies. The ASIC2 monomer is 59 kd. CNV, cytomegalovirus; eGFP, green fluorescent protein; HSV/EBV, herpes simplex virus-1/Epstein–Barr virus; IE, immediate early; RFP, red fluorescent protein.

were incubated with dox, RFP expression was turned on, indicating that the inducible transgenes were being expressed (**Figure 1b**).

Expression of mutant and wild-type human brain sodium channel

In order to monitor the expression of the ASIC2 channels, CHO cells were transfected with either pHET14B-ASIC2^{wt} or pHET14B-ASIC2^{G430F} amplicons in the presence of dox with and without amiloride to block the open channel. Sixteen h post-transfection cells were lysed and analyzed by western blotting (**Figure 1c**). A 59 kd band was observed in the cells expressing ASIC2^{wt}, in the presence or absence of amiloride. However, no band was observed in the ASIC2^{G430F}-expressing cells without amiloride, indicating the rapid and high toxicity of the mutant channel. When cells were transfected with pHET14B-ASIC2^{G430F} amplicon in the presence of dox and amiloride, expression of the mutant channel was detectable at a low level as compared to cells expressing ASIC2^{wt}, probably because amiloride does not completely block the mutant sodium current. In addition, after infection with the ASIC2^{wt}-encoding vector, cells immunostained for ASIC2, showing abundant expression of this channel protein (**Figure 1b**).

Measurement of sodium current

Gli36Gluc cells were infected with HET14B-ASIC2^{wt} or HET14B-ASIC2^{G430F} vectors, and 24 hours later, gene expression was induced with dox. Six hours postinduction, currents were recorded in whole-cell patch-clamp mode. Cells were held at −60 mV and given a voltage ramp stimulus every 1.2 seconds that changed the voltage from −100 to 100 mV in 200 ms. Amiloride was present in the bath to extend the life of the cells and improve seal formation on the cells. After recording background currents in the amiloride solution, the drug was washed out revealing a large inward current at negative potentials that had been blocked by

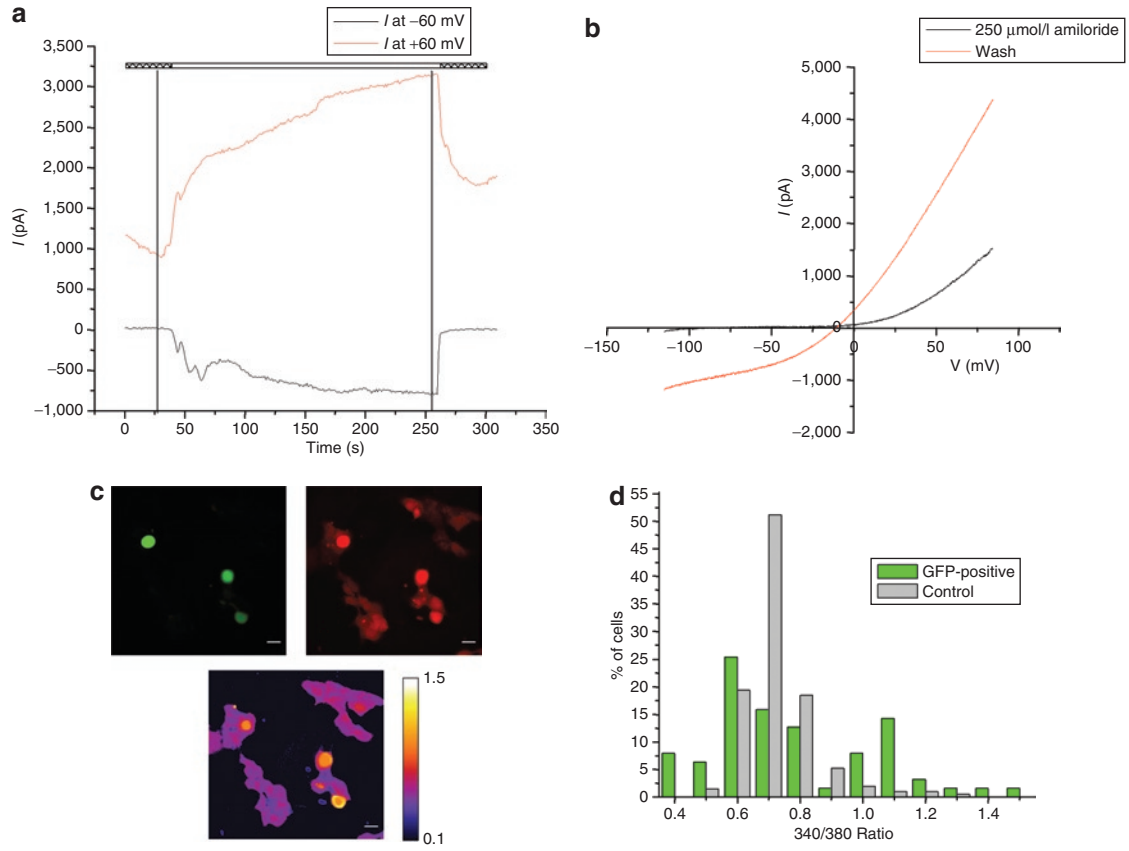

Figure 2 Monitoring of sodium influx in cells expressing the mutant ASIC2^{G430F} channel. Gli36 cells were infected with either HET14B-ASIC2^{wt} or HET14B-ASIC2^{G430F} amplicon vectors. Twenty four hours postinfection, cells were incubated with dox and analyzed for sodium influx 6–8 hours later. (**a**,**b**) Representative whole-cell patch-clamping on cells expressing ASIC2^{wt} or ASIC2^{G430F} channels. (**a**) Current over time at two voltages as determined by voltage sweeps (black trace at −60 mV and red trace at +60 mV). The hatched bars above show presence of 250 µmol/l amiloride in the bath and white bar shows switching to regular extracellular solution to wash off the amiloride block. (**b**) Current voltage graph determined by single voltage sweeps in either 250 µmol/l amiloride (black line, taken at first vertical line in **a**) or after washout (red line, taken at second vertical line in **a**). (**c**,**d**) Gli36Gluc cells were infected to express ASIC2^{G430F}. (**c**) Images are shown from the same field. Expression of enhanced GFP indicated 10% transduction efficiency (top left). Cells were incubated with dox to induce the mutant sodium channel expression. Six hours later, cells were loaded with SBFI-AM (top right, red) and the intracellular sodium was imaged in both ASIC2^{G430F}-expressing cell (GFP positive; $n = 63$) and nontransduced control cells (GFP negative; $n = 211$) by monitoring the SBFI ratio of fluorescence intensities at 340/380 nm using an Olympus IX81 microscope. False colors representation of SBFI excitation ratio values recorded in Gli36Gluc cells infected with HET14B-ASIC2^{G430F} showing the Na elevation in ASIC2^{G430F}-expressing cells (yellow cells) and not the nonexpressing cells [(**c**) bottom; purple cells]. (**d**) Distribution of cells at various 340/380 ratios. A significant increase in the number of cells with higher intracellular sodium levels were seen in cells expressing the ASIC2^{G430F} (GFP) as compared to nonexpressing control cells. [$^*P = 1.6 \times 10^{-11}$, χ^2-test comparing ASIC2^{G430F}-expressing cells (green) and control (nongreen cells)]. GFP, green fluorescent protein.

amiloride (Figure 2a,b). Amiloride was then washed back in to reblock the current. This current was seen in 7/8 eGFP-positive cells infected with the HET14B-ASIC2^{G430F} mutant channel vector and 0/5 eGFP-positive cells infected with the HET14B-ASIC2^{wt} wild-type channel vector. Similar results were obtained when the genes were delivered by transfection of amplicon DNA (data not shown).

Imaging of sodium entry

The influx of sodium via the mutant sodium channel in cultured cells was imaged using the sodium sensitive dye, SBFI-AM. Gli36 cells were infected with HSV/EBV amplicon vectors encoding either ASIC2^{wt} or ASIC2^{G430F} at a multiplicity of infection of 0.2 transducing units (tu) per cell (Figure 2c; top left, green cells). Transgene expression was turned on by addition of dox to the medium and 6 hours later cells were labeled with the cell permeable SBFI-AM (Figure 2c; top right, red cells). Sodium was imaged in individual cells in both ASIC2^{G430F}-expressing cells (GFP positive; $n = 63$) and nonexpressing cells (GFP negative; $n = 211$) by monitoring the SBFI ratio of fluorescence intensities at 340/380 nm using an Olympus IX81 microscope (Figure 2c; bottom and Figure 2d). A significant ($^*P = 1.6 \times 10^{-11}$, χ^2-test) increase in intracellular sodium levels was seen in most cells expressing the ASIC2^{G430F} mutant as compared to nonexpressing cells.

Killing effect of mutant ASIC2^{G430F} channels in culture

Tumor cells modified to stably express the naturally secreted Gaussia luciferase (Gluc) to assess viability[30,31] were used to monitor the killing effect of the mutant ASIC2^{G430F} channel. Gli36Gluc cells were infected with amplicon vectors expressing either HET14B-ASIC2^{wt} control or HET14B-ASIC2^{G430F} mutant channel and incubated with or without dox. Sixteen hours later, Gluc activity was assayed by taking aliquots of the conditioned medium, adding coelenterazine and measuring photon counts using a luminometer. A 70% decrease in Gluc activity in the medium was observed in cells infected with HET14B-ASIC2^{G430F} and induced with dox (Figure 3a), attributable to cell death as confirmed, using the WST-1 assay (Figure 3b). On the contrary, no loss in cell viability was seen in HET14B-ASIC2^{G430F}-infected cells which were not treated with dox or in HET14B-ASIC2^{wt}-infected cells in either the presence or absence of dox (Figure 3a,b). When these cultures were monitored 3 days later, there were no eGFP expressing cells remaining in the HET14B-ASIC2^{G430F}/dox treated cultures, corresponding to a >90% decrease in Gluc expression as compared to controls. We attribute the minimal "left-over" Gluc signal in the treated wells to glioma cells, which were not infected with the vector and were not adjacent to infected cells.

To evaluate whether HET14B-ASIC2^{G430F}-infected cells treated with dox had a bystander killing effect on uninfected cells, Gli36Gluc cells were infected with either HET14B-ASIC2^{G430F} or HET14B-ASIC2^{wt} vectors and mixed with Gli36 cells stably expressing firefly luciferase (Fluc) (Gli36Fluc)[32] in a 1:3 ratio, then replated in a 96-well plate at near confluency in the presence or absence of 65 µmol/l 18 α-glycyrrhetinic acid, an inhibitor of gap junctions. After 12 hours, wild-type and mutant sodium channel expressions were induced by dox and the bystander effect was assessed by measuring levels of Fluc in cell lysates 16 hours later. A 70% decrease in Gluc activity (corresponding to death of essentially all GFP$^+$ cells; data not shown) was observed in cells expressing ASIC2^{G430F} accompanied by a 35% decrease in Fluc activity in nonexpressing cells in these mixed populations, supporting a marked bystander effect (Figure 3c). In contrast, when the same cell mixture was replated in the presence of α-glycyrrhetinic acid, while a similar decrease in Gluc signal was observed, there was no detectable decrease in Fluc activity in these cultures (Figure 3c). On the other hand, mixtures of ASIC2^{wt}-expressing and nonexpressing cells in the same ratio showed no evidence of cell death in either population. To evaluate the extent of gap-junction communication in Gli36Gluc cells, we double-labeled the "donor" cells for 1 hour with the cell-permeant dye, acetoxymethyl ester calcein (Calcein-AM; green) to monitor the transfer through the gap junctions, and the cell-impermeant dye, DiI (red), to stain the cell membrane (Figure 3d top). These cells were then washed, and plated on top of a monolayer of nonlabeled Gli36 cells. After 4 hours, it was clear that calcein-AM had passed from the labeled cells (Calcein$^+$/DiI$^+$) to adjacent non-DiI-labeled cells at least two cell layers deep, as observed by fluorescence microscopy (Figure 3d bottom), proving that this tumor cell line forms gap junctions.

In order to image the killing effect of the mutant sodium channel in real time, Gli36Gluc cells infected with the HET14B-ASIC2^{G430F} vector, which encodes the mutant channel and eGFP, were treated with dox and placed in a 37 °C chamber on a confocal microscope and images were captured every 5 minutes over 12 hours. The ASIC2^{G430F}-expressing cells showed a marked change in shape from flat to round in ~3 hours (Figure 3e), suggesting that the sodium and water influx was in process and then appeared to swell and burst (**Supplementary Video S1**). Within 12 hours, essentially, all infected green cells had disappeared as well as most adjacent noninfected nongreen cells, confirming the bystander killing effect of this system (Figure 3e and **Supplementary Video S1**). Interestingly, no red fluorescent signal was seen in the ASIC2^{G430F}-expressing cells, which probably reflects a combination of the delayed production of this RFP and rapid killing, after expression of a few mutant channels, so that there was not sufficient time to generate enough dsRed protein for a fluorescent signal. When the same experiment was repeated with cells infected with vector expressing the wild-type channel and eGFP, no toxic effect was observed at any time due to expression of the wild-type channel; expression of dsRed was robust after 12 hours (Figure 3e**;** cells appear yellow due to coexpression of eGFP and RFP), and these cells survived for over a week without any signs of toxicity (data not shown).

To evaluate the mutant sodium channel for therapy of multiple tumor cell types, B16-F0 mouse melanoma cells, BT-20 human breast carcinoma, A549 human lung carcinoma, LNCaP human prostate adenocarcinoma, and HeLa human cervix adenocarcinoma were modified to express Gluc as described.[30] Cells were plated in 96-well plates and infected with vectors expressing ASIC2^{wt} (control) or ASIC2^{G430F}, and ASIC2 expression was induced with dox. Twenty-four hours later, an aliquot of the conditioned medium was assayed for Gluc activity. A 70–80% decrease in Gluc activity was observed in all ASIC2^{G430F} treated wells as compared to control vector, proving that this therapeutic

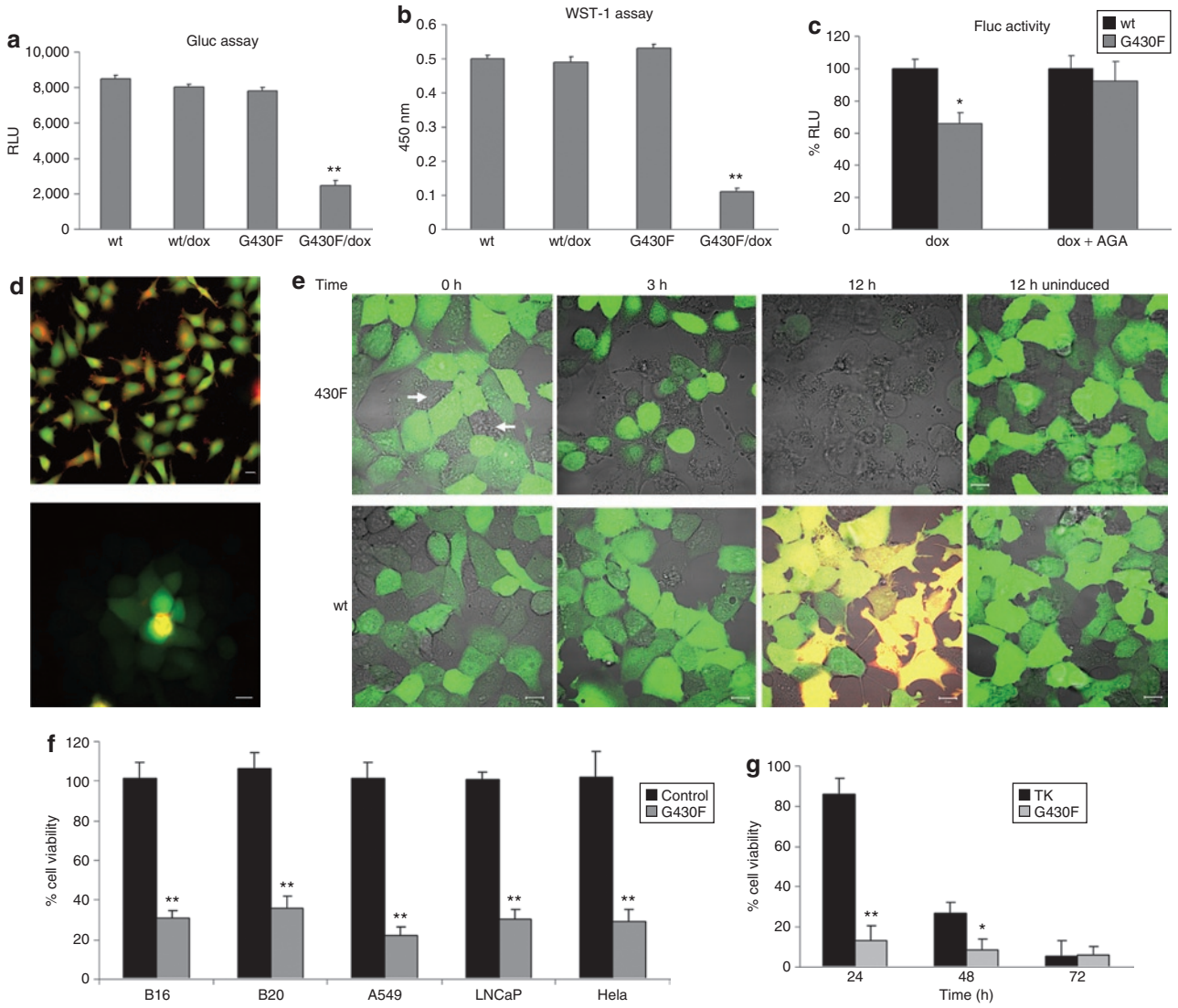

Figure 3 Tumor cell death caused by expression of the mutant ASIC2^{G430F} sodium channel. Gli36Gluc cells were infected with the amplicon vectors carrying the expression cassettes for either wild-type ASIC2^{wt} or the mutant ASIC2^{G430F} channel. (**a**) Sixteen hours postinfection and dox treatment, 10 µl aliquots of the conditioned medium were analyzed for Gluc activity as a measure of cell viability. (**b**) WST-1 viability assay was carried out in the same wells used for Gluc assessment, confirming cell death only in the ASIC2^{G430F} + dox wells. (**c**) To assess the bystander killing effect, cells infected with vector encoding either the wild type ASIC2^{wt} or mutant ASIC2^{G430F} channel were mixed in a 1:3 ratio with noninfected Gli36Fluc cells and plated together as a monolayer in the presence or absence of AGA, an inhibitor of gap junctions, and then gene expression was induced with dox. Sixteen hours later, cells were lysed and analyzed for Fluc activity. (**d**) To evaluate gap junctional communication between Gli36Gluc cells, these cells were labeled with both Calcein-AM (green) and DiI (red) (top panel) and plated on top of a monolayer of nonlabeled cells (lower panel). Four hours later, clear transfer of the Calcein-AM dye to non-DiI-labeled cells was evident, supporting transfer through functional gap junctions. (**e**) Cells were infected with HET14B-ASIC2^{G430F} or HET14B-ASIC2^{wt} vectors and 24 hours later were placed in a 37 °C chamber on a confocal microscope and images were captured every 5 minutes over 12 hours after adding dox to the medium. Cells expressing the mutant channel as well as neighboring noninfected cells (arrows) became round 3 hours after induction with dox, indicating sodium and water influx, and were completely lysed by 12 hours with no sign of dsRed expression. On the contrary, the cells expressing the wild-type channel did not show any signs of toxicity and were positive for both dsRed and green fluorescent protein (yellow) by 12 hours after dox treatment. (**f**) Different types of tumor cells expressing Gluc were infected with HET14B-ASIC2^{G430F} or HET14B-ASIC2^{wt} control vector and incubated with dox. Twenty four hours later, an aliquot of the conditioned medium was assayed for Gluc activity. (**g**) Gli36Gluc cells were infected with either HET14B-ASIC2^{G430F} or herpes simplex virus-TK amplicon vectors and treated with dox or ganciclovir, respectively. At different time points, aliquots of the conditioned medium were assayed for Gluc activity. Results are expressed as percentage, in which the control cells of each type were set at 100%. In **a–c** and **f,g**, values are given as the mean ± SD with $^{**}P < 0.001$ and $^{*}P < 0.005$ as calculated by two-tailed Student's *t*-test. AGA, α-glycyrrhetinic acid; TK, thymidine kinase.

strategy can be used for the treatment of different tumor types (Figure 3f).

To compare the potency of this new killing modality to a well-established gene therapy mode, we packaged HSV amplicon vectors encoding the HSV thymidine kinase (TK) under the cytomegalovirus promoter (provided by Cornel Fraefel, Institute of Virology, University of Zurich, CH). Gli36Gluc cells were infected with either HET14B-ASIC2^{G430F} or HSV-TK vectors (multiplicity of infection of 0.5) and 6 hours later, cells were washed and treated with either dox or ganciclovir (GCV), respectively. Cell viability

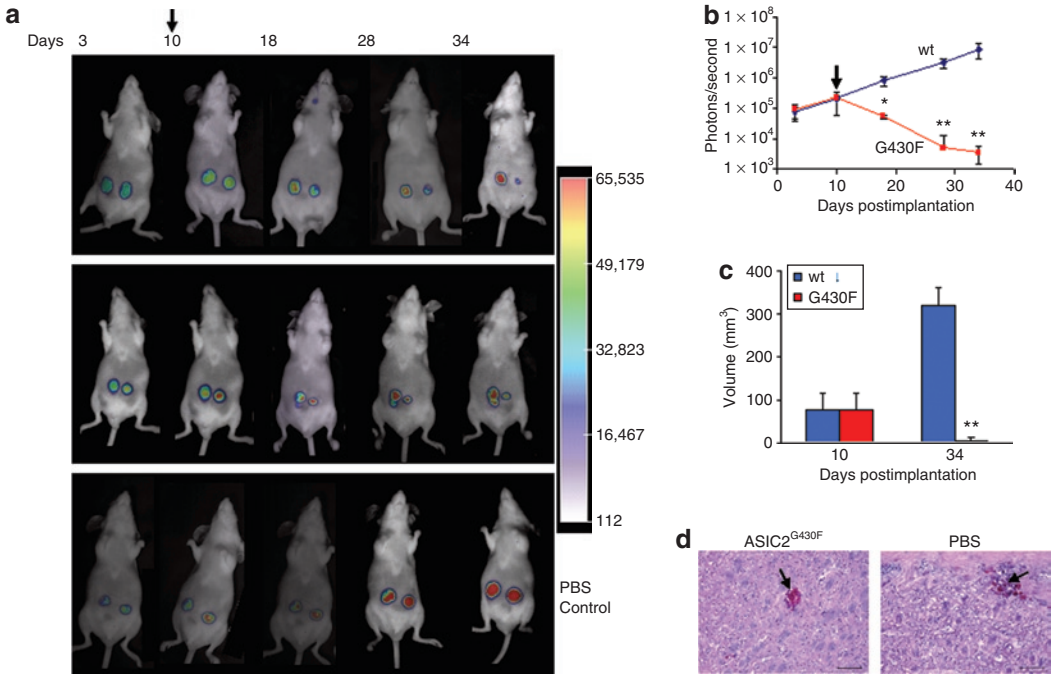

Figure 4 ***In vivo*** **tumor therapy with herpes simplex virus-1/Epstein–Barr virus amplicon vector encoding ASIC2^{G430F} mutant sodium channel.** (**a**) Gli36Gluc cells were implanted subcutaneously in both flanks of nude mice. Ten days postimplantation (arrow) when tumors were ~80 mm^3, the left side tumor received intratumoral injection of the vector carrying the expression cassette for the ASIC2^{wt} control channel and the right side received vector with the expression cassette for the ASIC2^{G430F} mutant channel (10^5 tu in 10 µl/tumor). Dox (400 µg/ml with 5% sucrose) was included in the mice drinking water after the first injection. Two representative animals from this group are shown over time (top and middle panels). In another control group, both tumors were injected with PBS (bottom panel). Tumor growth and response to therapy was monitored over time by *in vivo* Gluc bioluminescence after intravenous injection of coelenterazine and acquisition of photon counts using a charge-coupled device camera. (**b**) Tumor volumes were quantitated by photon counting and averaging over tumors in the ASIC2^{wt} and ASIC2^{G430F} vector-treated animals ($n = 5$ per group). Mean photon counts ± SD are shown. Arrow indicates time of first vector injection. Asterisk indicates a level of significance of $^*P < 0.005$ and $^{**}P < 0.001$ (calculated by Student's *t*-test) between tumors treated with control and mutant vectors. (**c**) Caliper measurements of tumor diameter converted to volume immediately before vector injection (10 days postimplantation) and at the last time point of the experiment (34 days postimplantation) ($^{**}P < 0.001$). (**d**) Amplicon vector (1 µl; 2×10^4 tu) expressing ASIC2^{G430F} or PBS were stereotactically injected into the striatum of nude mice brain. Dox was included in the drinking water immediately after injection. Three days postinjection, mice were killed and brains were removed, postfixed in paraformaldehyde and formalin/sucrose, frozen, and sectioned into 20 µm sections. Sections were mounted on slides and evaluated by hematoxylin and eosin staining. Arrow shows the injection site. Bar = 100 µm. PBS, phosphate-buffered saline.

was monitored as Gluc activity in the conditioned medium at different time points. The mutant ASIC2 channel produced around 80% cell death at 24 hours postinfection as compared to <10% with TK/GCV at the same time point. At 48 hours postinfection, there was >90% cells death with ASCI2 mutant channel as compared to 70% cell death with TK/GCV, and by 72 hours both treatments showed similar killing (>90%). These results show that the mutant ASIC2 channel has the advantage of a more rapid killing effect as compared to TK. Additional advantages are that the mutant ASIC2 channel become equally toxic to dividing and nondividing tumor cells, while the TK/GCV killing mechanism depends on DNA replication, and that the mutant channel is regulated by a drug-inducible promoter, while the *TK* gene is typically not.

ASIC2^{G430F} mutant sodium channel for *in vivo* tumor therapy

In order to evaluate the effectiveness of the ASIC2^{G430F} mutant sodium channel for tumor therapy *in vivo*, we used Gli36Gluc cells as a model since these cells have been shown previously to form reproducible tumors when implanted subcutaneously in nude mice.[31,32] Gli36Gluc cells were implanted subcutaneously in flanks of nude mice on the left and right sides. Tumor growth was monitored over time by *in vivo* bioluminescence imaging of Gluc activity after intravenous injection of coelenterazine and signal acquisition using a charge-coupled device camera. At day 10, when tumors reached around 80 mm^3 in volume, as estimated by caliper measurements, mice were separated randomly into two groups. In one group, tumors on the right side were injected with 10^5 transducing units (tu) HSV/EBV hybrid amplicon vector (in 10 µl) carrying the expression cassette for the ASIC2^{G430F} mutant sodium channel and tumors on the left side were injected with similar tu and volume of the control vector carrying the expression cassette for the ASIC2^{wt} wild-type channel. In another group of mice, both tumors received phosphate-buffered saline (PBS) injections. These intratumoral injections were repeated once every day for three consecutive days. Doxycycline (400 µg/ml with 5% sucrose) was included in the drinking water starting from the day of the first vector injection. Tumor growth and the response to mutant sodium channel therapy were monitored once every week over one month by *in vivo* bioluminescence imaging for Gluc and by caliper measurements. A marked decrease in Gluc activity was observed in tumors injected with the HET14B-ASIC2^{G430F} vector expressing the

mutant sodium channel starting within the first week after vector injection and dox exposure, with continuing regression in tumor size over 34 days of observation (**Figure 4a,b**). Tumors in the same animals injected with control vector expressing the ASIC2^{wt} as well as tumors in control group injected with PBS continued to increase in size over this period as assessed by bioluminescence imaging (**Figure 4a,b**). Tumor size was confirmed by caliper measurements with a decrease in size by >90% for tumors expressing the mutant channel by 34 days after the 3 day treatment period, while tumors expressing the normal channel or control tumors increased in size by 325% over this period (**Figure 4c**). This *in vivo* therapeutic experiment was repeated and treated mice were followed for 2 months. We observed that the tumors treated with the amplicon vector expressing ASIC2^{G430F} and treated with dox regressed as mentioned previously and did not regrow (data not shown). To assess the effect of the expression of the mutant sodium channel on normal cells, 2×10^4 tu of the HET14B-ASIC2^{G430F} vector or PBS were injected sterotactically into the striatum of nude mice brain using the following coordinates from bregma in mm: (AP +0.5, ML +2.0, DV −2.5), as described.[32] Dox was included in the drinking water immediately after injection. Three days postinjection, mice were killed and brains were removed, postfixed in paraformaldehyde and formalin/sucrose, frozen, and sectioned into 20 µm sections. Sections were mounted on slides and evaluated by fluorescence microscopy for eGFP and by hematoxylin and eosin staining as described.[33] No GFP positive cells were observed showing that the infected cells died, however, there was no apparent sustained damage to the normal brain cells surrounding the injection site, except some bleeding at the needle track, probably due to minimal gap junction connections among normal cells (**Figure 4d**). When the same vector was injected into the leg muscles in mice, similar results were obtained (data not shown).

DISCUSSION

This study describes a novel method for killing tumor cells using a mutant ASIC2 channel subunit under a tightly controlled drug-inducible promoter (tet-on) delivered by an HSV amplicon vector. This mutant ASIC2 subunit can coassemble with other mutant subunits or with wild-type ASIC2 subunits to form an open channel that allows an unrestricted and lethal flow of sodium into cells. Different tumor cell types infected with vector encoding the mutant channel were observed to swell and burst within hours after inducing expression of the mutant channel, indicating inflow of water with sodium, while expression of the wild-type channel had no effect on cell viability. Sodium influx through this mutant channel was confirmed by patch-clamp recording with amiloride blockade, and visualized directly using the fluorescent Na^+ indicator SBFI-AM esters. Importantly, there was a bystander killing effect that was several cell layers deep, presumably mediated by sodium influx into adjacent cells via gap junctions, visualized using the fluorescent dye, Calcein-AM. Direct injection of the vector encoding the mutant channel into subcutaneous tumors with coadministration of dox resulted in marked regression of the tumor mass over the following 3 weeks, with no regrowth over 2 months. This tumor killing strategy provides a means to rapidly debulk tumor mass by injection rather than surgical removal of tissue with drug-regulated induction and little-to-no toxicity to normal cells.

Death causing mutations in the superfamily of DEG/ENaC channels to which ASIC2 belongs were first identified by random mutagenesis of *Caenorhabditis elegans* and mutations similar to G430F cause neuronal degeneration and muscle hypercontraction.[24,25] Human channel proteins, ASIC1, and ASIC2 are expressed by most central and peripheral neurons, although mutant forms of these mammalian homologs have not been shown to cause neurodegeneration.[20] However, the known channel-opening effects of the mutations found in nematode neurons provided the basis for their use in cancer therapy, a dramatic example of research in simple organisms leading to innovative therapeutic modalities for human disease.

Currently, several hundred gene therapy protocols have been approved and tested in clinical phase I–III trials, most using viral vectors for cancer (http://www.wiley.co.uk/genetherapy/clinical/). Effective gene therapy requires efficient delivery of the therapeutic gene to tumor cells and a bystander effect such that the neighboring nontransduced tumor cells are also killed. Optimization of gene therapy has been facilitated by imaging methods, which provide a means to monitor transgene expression, cell specificity and duration, and tumor growth and regression.[34,35] Only a few of the gene therapy strategies for cancer have targeted ion channels. Glioma cells express a novel voltage-activated chloride current that is reportedly blocked by the scorpion toxin, chlorotoxin,[36] which in turn binds matrix metalloproteinase-2 on these tumor cells.[37] Treatment of glioma cells with this toxin inhibits their proliferation and migration, while astrocytes are not affected.[37] In a phase 1 trial for glioblastoma, radioactively labeled chlorotoxin was found to have no dose-limiting toxicity and to permit γ-imaging of its distribution throughout the body.[11] This toxin is of special interest with respect to the mutant sodium channel used in this article as gliomas grow in tissue with high water content (peritumoral edema) and depend on chloride channels, as well as K^+ Cl^- (KCC) cotransporters, to regulate their cell volume.[38] Thus, the toxicity of the mutant sodium channel might be increased by reducing the ability of tumor cells to regulate water intake through treatment with chlorotoxin to block the chloride channel or with (dihydroindenyl)oxyalkanoic acid to block the KCC cotransporter.[39]

Another ion transporter used for tumor therapy has been the sodium iodide symporter, which normally mediates transport of iodide into thyroid cells. In this approach, sodium iodide symporter is expressed in tumor cells in combination with ^{131}iodide,[40] but high levels of ^{131}iodide are needed to exert a cytotoxic effect. The therapeutic efficacy for tumor cells has been improved by codelivery of thyroperoxidase, which catalyzes the oxidation of iodide promoting binding to tyrosine residues on thyroglobulin,[41] or of thyroid transcription factor-1 to promote expression of thyroid specific proteins which bind iodide.[42] Sodium iodide symporter transgene expression can be imaged by ^{124}I positron emission tomography/computed tomography and a ^{123}I planar gamma camera in animal models.[43]

Therapeutic advantages of ASIC2^{G430F} mutant sodium channel for tumor therapy include a rapid killing mechanism that would be effective against both dividing and non-dividing tumor cells, as well as a strong bystander effect. Safety features include drug-inducible regulation of the transgene and a limiting effect through dilution of

ions/water as they spread among cells through gap junctions, combined with delivery by intratumoral injection of the vector. ASICs are normally expressed in human gliomas,[44] which form gap junctions with each other as well as astrocytes and endothelial cells in the brain.[45] The gap junctions between glioma cells and astrocytes are involved in glioma cell migration,[44] ergo death of these "guide" astrocytes might restrict glioma cell migration. Death of neighboring endothelial cells might also reduce tumor angiogenesis. Given the rapid killing mechanism of this mutant sodium vector with subsequent degradation of vector and transgene proteins, it seems unlikely that an immune response to the vector would reduce its effectiveness in an immune competent host.

The mutant human brain sodium channel described here provides a robust killing mechanism for tumor cells by a rapid, explosive mechanism. This potent killing channel could be inserted into any virus vector provided expression could be controlled during packaging of the vector, with adenovirus and lentivirus vectors also having the potential for tight transgene regulation delivery.[46] For all tumor types, additional therapeutic effect might be achieved by coexpression of connexin-43 to increase the number of gap junctions, a strategy used to increase passage of GCV-derived nucleotides from tumor cells expressing viral TK to neighboring tumor cells.[47] In addition to being an adjunct therapy for malignant tumors, mutant ASIC2 therapy may also prove effective in shrinking benign tumors in inoperable locations, such as meningiomas or schwannomas pressing on critical neural structures, or in removing portions of malignant tumors that are in inoperable locations.[48]

MATERIALS AND METHODS

Cell culture. The Gli36 human glioma cell line was obtained from Anthony Capanogni, University of California (Los Angeles, CA); Vero 2-2 African green monkey kidney cells from Rozanne Sandri-Goldin, University of California (Irvine, CA); CHO-K1 Chinese-Hamster-Ovary cells, B16-F0 mouse skin melanoma, BT-20 human breast carcinoma, A549 human lung carcinoma, LNCaP human prostate adenocarcinoma and HeLa human cervix adenocarcinoma were purchased from the American Type Tissue Collection (ATCC, Manassas, VA). Cells were transduced to stably express the naturally secreted Gluc or Fluc as previously described.[31] All cells were cultured as per ATCC instructions in medium, supplemented with 10% fetal bovine serum (Sigma), 100 U penicillin, and 0.1 mg streptomycin (Sigma) per milliliter at 37 °C in a 5% CO_2 humidified incubator.

HSV/EBV hybrid amplicon vector construct. The pHET-14B amplicon is an HSV/EBV hybrid vector, which consists of the HSV-1 amplicon backbone (containing two noncoding elements of HSV—an origin of DNA replication, *oriS* and a virion packaging signal, *pac*), the EBV origin of replication (oriP), and a mutant *EBNA-1* gene[49] with cassettes encoding tet-silencer and activator proteins[27] under the cytomegalovirus promoter and a bidirectional tet-responsive promoter[28] driving the expression of dsRed as well as the channel transgenes (**Figure 1**). This hybrid amplicon plasmid also contains an eGFP cassette (Clontech) under the control of HSV-1 IE4/5 promoter. The cDNA sequences encoding the wild-type ASIC2 or mutant ASIC2^{G430F} form of the human ASIC2 channel were amplified by polymerase chain reaction from plasmids[50] and cloned in pHET-14B in the NotI site to generate pHET14B-ASIC2^{wt} or pHET14B-ASIC2^{G430F}. All amplicon constructs were packaged in HSV-1 virions using a helper virus-free packaging system, as described.[29]

Luciferase activity. Gluc activity was measured by adding 20 µmol/l coelenterazine (Prolume/Nanolight) to an aliquot (typically 10 µl) of the cell-free conditioned medium and photon counts were acquired for 10 seconds using a luminometer (Dynex). For Fluc detection, cells were lysed in 1× RLB buffer (Promega) and 450 µmol/l Beetle D-luciferin (Molecular Imaging Products) was added directly to the cell lysates in a 96-well plate and photon counts were acquired, as mentioned previously.

Western blot. CHO-K1 cells were transfected with 2 µg of either pHET14B-ASIC2^{wt} or pHET14B-ASIC2^{G430F} using lipofectamine in the presence of 1 µg/ml doxycycline (Sigma). Total cell lysates were prepared at different time points in lysis buffer containing 150 mmol/l NaCl, 50 mmol/l TRIS, pH 8.0, 1% NP-40, 0.5% deoxycholate, 0.1% sodium dodecyl sulfate, and protease inhibitors (PI Complete; Boehringer, Mannheim). Protein (40 µg) was electrophoresed in 12.5% sodium dodecyl sulfate-polyacrylamide gels and transferred to nitrocellulose membranes (Bio-Rad). Membranes were blocked overnight in 10% nonfat milk powder in TBST (150 mm NaCl, 50 mm TRIS, pH 7.9, 0.5% TWEEN) and probed with a rabbit anti-ASIC2 antibody (R6798)[50] diluted in TBST overnight at 4 °C. Membranes were then washed and incubated with horseradish peroxidase conjugated to secondary antibodies: sheep anti-mouse immunoglobulin G-horseradish peroxidase (1:5,000; Amersham Pharmacia Biotech). Protein was detected using SuperSignal West Pico Chemiluminescent Substrate (Pierce).

Immunocytochemistry. CHO-K1 cells were transfected with pHET14B-ASIC2^{wt} as above, in the presence of dox, and 24 hours later, cells were replated on coverslips. Twenty-four hours after replating, cells were fixed with 4% paraformaldehyde in PBS for 10 minutes at room temperature, washed with PBS and permeabilized with 0.1% NP-40 in PBS for 10 minutes. Blocking was performed using 10% goat serum (Vector Laboratories) and 1% BSA (Sigma) in PBS for 1 hour. Cells were incubated with rabbit anti-ASIC2 antibody (1:100) overnight at 4 °C. For fluorescence detection, we used an affinity pure donkey anti-rabbit antibody conjugated to Alexa660 (1:200; Invitrogen). Coverslips were mounted onto slides using gelvatol mounting medium. Images were captured using an inverted fluorescent microscope (Nikon TE 200-U) coupled to a digital camera.

Sodium imaging in culture. Gli36Gluc cells were infected with either HET14B-ASIC2^{wt} or HET14B-ASIC2^{G430F} vector, as mentioned previously, and cultured in the presence of 1 µg/ml doxycycline. Eight hours later, cells were loaded for 1 hour with 10 µg/ml of the sodium sensitive dye SBFI-AM, a cell permeable acetoxy methyl ester of a benzofuran isophthalate derivative (Molecular Probes). Intracellular sodium was imaged by monitoring the ratio of the fluorescence intensity obtained by exciting SBFI at 340 and 380 nm while monitoring emission at 500 nm using a Olympus IX81 equipped with a Fura-2 filter set.

Electrophysiology/patch clamping. Gli36Gluc cells were either transfected with pHET14B-ASIC2^{wt} or pHET14B-ASIC2^{G430F} amplicon DNA using lipofectamine or infected with the corresponding amplicon vectors, and gene expression was induced with doxycycline, as mentioned earlier. Six hours post-transduction, cells were observed using an IM-35 microscope (Zeiss) to identify eGFP-positive cells for recording. Cells were placed in an extracellular solution containing (in mmol/l): 140 NaCl, 5 KCl, 2 $CaCl_2$, 1 $MgCl_2$, 10 HEPES, pH 7.4, osmolarity 340 mOsm. Amiloride (250 µmol/l; Sigma) was added to this solution for blocking experiments. Patch pipettes were pulled to 2–4 MΩ from R6 glass (Garner Glass). Pipettes were filled with internal solution containing (in mmol/l): 140 KAspartate, 10 NaCl, 4 $MgCl_2$, 5 EGTA, 10 HEPES, 4 Na_3ATP, 0.3 Li_3GTP, 0.1 $CaCl_2$, pH 7.4, osmolarity 315 mOsm. Cells were studied in the whole-cell voltage-clamp mode with an Axopatch 200A amplifier holding at −60 mV. The stimulus waveform was controlled by pClamp 9.0 software (Axon Instruments) and responses digitized using a Digidata 1322A (Axon Instruments). Data analysis and fitting were done with Origin 6.0 (Microcal Software). A voltage ramp protocol that changed the voltage from −100 mV to 100 mV in 200 ms was used to measure currents in the cells. The voltage was later corrected for liquid junction potentials offline. Solutions were exchanged in the chamber using an eight channel ValveLink system (AutoMate Scientific).

Monitoring of gap junctions. Gli36 cells were plated in 24-well plates. Twenty-four hours later, cells were washed and incubated with 5 µmol/l Calcein-AM, 10 µmol/l DiI and 50% pluronic acid (all from Molecular Probes) for 1 hour at 37 °C. Monolayers were then rinsed and cells were washed of the plate and added to another well containing a monolayer of unlabeled Gli36 cells. Calcein-AM transfer from labeled cells to nonlabeled cells was monitored using fluorescence microscopy.

Live cell imaging. Gli36Gluc cells were infected with either HET14B-ASIC2^{wt} or HET14B-ASIC2^{G430F} amplicon vectors, as mentioned previously, at a multiplicity of infection of 0.5. Cells were rinsed with PBS and growth medium containing 1 µg/ml dox was added to the cells 24 hours postinfection. Real-time fluorescence images were acquired either at different time points or every 5 minutes for 12 hours using a Nikon TE300 microscope and Biorad MRC 100 Laser Confocal Imaging System.

In vivo *tumor model.* Gli36Gluc cells (10^6) were implanted subcutaneously into the left and right flanks of nude mice (five mice/group; 6 weeks of age, weighing 25–27 g), which were anesthetized by intraperitoneal injection of a mixture of ketamine (25 g/l) and xylazine (5 g/l). Tumor volume was monitored on a weekly basis by *in vivo* bioluminescence imaging after intravenous injection of coelenterazine (4 mg/kg body weight in 150 µl PBS) and acquisition of photon counts for 5 minutes using a cooled charge-coupled device camera (Roper Scientific), as described.[31] At day 10 postimplantation, in one group of five mice, all tumors on the left side were injected with 10^5 tu (in 10 µl) HET14B-ASIC2^{wt} control vector and tumors on the right side were injected with similar tu and volume of HET14B-ASIC2^{G430F} vector. A control group of five mice received PBS injection in both tumors. Doxycycline (400 µg/ml) as well as sucrose (5%) were included in the drinking water right after vector injection and thereafter. Vector injections were repeated in total three times on three consecutive days. Tumor growth and response to the mutant sodium channel therapy was monitored by *in vivo* bioluminescence imaging as mentioned earlier, using the charge-coupled device camera. Conventional white-light surface images were obtained immediately before each photon counting session to provide an anatomical outline of the animal. Following data acquisition, postprocessing and visualization were performed using CMIR-Image, a custom-written program with image display and analysis suite developed in IDL (Research Systems). Images were displayed as a pseudo-color photon count image, superimposed on a gray-scale anatomic white-light image, allowing assessment of both bioluminescence intensity and its anatomical source. Regions of interest were defined using an automatic intensity contour procedure to identify bioluminescent signals with intensities significantly greater than background. The sum of the photon counts in these regions was then calculated. The same animal experiment was repeated once more to obtain statistical significance for a total of 10 mice/group.

SUPPLEMENTARY MATERIAL

Video S1.

ACKNOWLEDGMENTS

We thank Dr Bujard for providing tetracycline regulatory elements used in the amplicon vector and Dr Fraefel for providing the HSV-TK amplicon plasmid; Dr Rachamimov (Pathologist at MGH) for analyzing the hematoxylin and eosin stained sections. Nicole Lewandrowski, Juliet Fernandez, Ozlem Senol, and Johanna M. Niers for technical help; Dr Yellen for access to the sodium imaging microscope; Suzanne McDavitt for skilled editorial assistance; and Igor Bagayev for assistance with confocal microscopy. This work was supported by grants from the National Cancer Institute (CA69246 and CA86355 to XOB and RW, and 1K99CA126839 to BAT), from NINDS (NS44363 to JG-A) and from the Brain Tumor Society (to B.A.T. and X.O.B.). D.P.C. is an Investigator of the Howard Hughes Medical Institute.

REFERENCES

1. Chiocca, EA, Broaddus, WC, Gillies, GT, Visted, T and Lamfers, ML (2004). Neurosurgical delivery of chemotherapeutics, targeted toxins, genetic and viral therapies in neuro-oncology. *J Neurooncol* **69**: 101–117.
2. Lam, YP and Breakefield, XO (2001). Potential of gene therapy for brain tumors. *Hum Mol Genet* **10**: 777–787.
3. Yang, ZR, Wang, HF, Zhao, J, Peng, YY, Wang, J, Guinn, BA *et al.* (2007). Recent developments in the use of adenoviruses and immunotoxins in cancer gene therapy. *Cancer Gene Ther* **14**: 599–615.
4. Hodi, FS and Dranoff, G (2006). Combinatorial cancer immunotherapy. *Adv Immunol* **90**: 341–368.
5. Ochsenbein, AF (2002). Principles of tumor immunosurveillance and implications for immunotherapy. *Cancer Gene Ther* **9**: 1043–1055.
6. Aghi, M, Hochberg, F and Breakefield, XO (2000). Prodrug activation enzymes in cancer gene therapy. *J Gene Med* **2**: 148–164.
7. Schepelmann, S and Springer, CJ (2006). Viral vectors for gene-directed enzyme prodrug therapy. *Curr Gene Ther* **6**: 647–670.
8. Zhang, L and Fang, B (2005). Mechanisms of resistance to TRAIL-induced apoptosis in cancer. *Cancer Gene Ther* **12**: 228–237.
9. Dingli, D, Russell, SJ and Morris, JC (2003). *In vivo* imaging and tumor therapy with the sodium iodide symporter. *J Cell Biochem* **90**: 1070–1086.
10. Ljunggren, K, Liu, X, Erlandsson, K, Ljungberg, M, Salford, L and Strand, SE (2004). Absorbed dose distribution in glioma tumors in rat brain after therapeutic intratumoral injection of 201Tl-chloride. *Cancer Biother Radiopharm* **19**: 562–569.
11. Mamelak, AN, Rosenfeld, S, Bucholz, R, Raubitschek, A, Nabors, LB, Fiveash, JB *et al.* (2006). Phase I single-dose study of intracavitary-administered iodine-131-TM-601 in adults with recurrent high-grade glioma. *J Clin Oncol* **24**: 3644–3650.
12. Hampl, J, Brown, A, Rainov, N and Breakefield, XO (2001). Methods for gene delivery to neural tissue. In: Chin, HR, Moldin, SO (eds). *Methods in Genomic Neuroscience.* CRC Press: Baton Rouge, FL, pp. 229–265.
13. Vähä-Koskela, MJ, Heikkilä, JE and Hinkkanen, AE (2007). Oncolytic viruses in cancer therapy. *Cancer Lett* **254**: 178–216.
14. Hadaczek, P, Kohutnicka, M, Krauze, MT, Bringas, J, Pivirotto, P, Cunningham, J *et al.* (2006). Convection-enhanced delivery of adeno-associated virus type 2 (AAV2) into the striatum and transport of AAV2 within monkey brain. *Hum Gene Ther* **17**: 291–302.
15. McKee, TD, Grandi, P, Mok, W, Alexandrakis, G, Insin, N, Zimmer, JP *et al.* (2006). Degradation of fibrillar collagen in a human melanoma xenograft improves the efficacy of an oncolytic herpes simplex virus vector. *Cancer Res* **66**: 2509–2513.
16. Shah, K and Breakefield, X (2006). HSV amplicon vectors for cancer therapy. *Curr Gene Ther* **6**: 361–370.
17. Hampl, JA, Camp, SM, Mydlarz, WK, Hampl, M, Ichikawa, T, Chiocca, EA *et al.* (2003). Potentiated gene delivery to tumors using herpes simplex virus/Epstein-Barr virus/RV tribrid amplicon vectors. *Hum Gene Ther* **14**: 611–626.
18. Wang, S and Vos, JM (1996). A hybrid herpesvirus infectious vector based on Epstein-Barr virus and herpes simplex virus type 1 for gene transfer into human cells *in vitro* and *in vivo*. *J Virol* **70**: 8422–8430.
19. Wang, S, Fraefel, C and Breakefield, XO (2002). HSV-1 amplicon vectors. In: Philips, I (ed.). *Methods in Enzymology, Gene Therapy Methods*. pp. 593–603.
20. García-Añoveros, J, Derfler, B, Neville-Golden, J, Hyman, BT and Corey, DP (1997). BNaC1 and BNaC2 constitute a new family of human neuronal sodium channels related to degenerins and epithelial sodium channels. *Proc Natl Acad Sci USA* **94**: 1459–1464.
21. Jasti, J, Furukawa, H, Gonzales, EB and Gouaux, E (2007). Structure of acid-sensing ion channel 1 at 1.9 A resolution and low pH. *Nature* **449**: 316–323.
22. Waldmann, R, Champigny, G, Voilley, N, Lauritzen, I and Lazdunski, M (1996). The mammalian degenerin MDEG, an amiloride-sensitive cation channel activated by mutations causing neurodegeneration in *Caenorhabditis elegans*. *J Biol Chem* **27**: 10433–10436.
23. García-Añoveros, J, García, JA, Liu, JD and Corey, DP (1998). The nematode degenerin UNC-105 forms ion channels that are activated by degeneration- or hypercontraction-causing mutations. *Neuron* **20**: 1231–1241.
24. Chalfie, M and Wolinsky, E (1990). The identification and suppression of inherited neurodegeneration in *Caenorhabditis elegans*. *Nature* **345**: 410–416.
25. García-Añoveros, J, Ma, C and Chalfie, M (1995). Regulation of *Caenorhabditis elegans* degenerin proteins by a putative extracellular domain. *Curr Biol* **5**: 441–448.
26. Bragg, DC, Camp, SM, Kaufman, CA, Wilbur, JD, Boston, H, Schuback, DE *et al.* (2004). Perinuclear biogenesis of mutant torsin-A inclusions in cultured cells infected with tetracycline-regulated herpes simplex virus type 1 amplicon vectors. *Neuroscience* **125**: 651–661.
27. Freundlieb, S, Schirra-Müller, C and Bujard, H (1999). A tetracycline controlled activation/repression system with increased potential for gene transfer into mammalian cells. *J Gene Med* **1**: 4–12.
28. Baron, U, Freundlieb, S, Gossen, M and Bujard, H (1995). Co-regulation of two gene activities by tetracycline via a bidirectional promoter. *Nucleic Acids Res* **23**: 3605–3606.
29. Saeki, Y, Breakefield, XO and Chiocca, EA (2003). Improved HSV-1 amplicon packaging system using ICP27-deleted, oversized HSV-1 BAC DNA. *Methods Mol Med* **76**: 51–60.
30. Badr, CE, Hewett, JW, Breakefield, XO and Tannous, BA (2007). A highly sensitive assay for monitoring the secretory pathway and ER stress. *PLoS ONE* **2**: e571.
31. Tannous, BA, Kim, DE, Fernandez, JL, Weissleder, R and Breakefield, XO (2005). Codon-optimized Gaussia luciferase cDNA for mammalian gene expression in culture and *in vivo*. *Mol Ther* **11**: 435–443.
32. Wurdinger, T, Badr, C, Pike, L, de Kleine, R, Weissleder, R, Breakefield, XO *et al.* (2008). A secreted luciferase for *ex vivo* monitoring of *in vivo* processes. *Nat Methods* **5**: 171–173.
33. Aboody, KS, Brown, A, Rainov, NG, Bower, KA, Liu, S, Yang, W *et al.* (2000). Neural stem cells display extensive tropism for pathology in adult brain: evidence from intracranial gliomas. *Proc Natl Acad Sci USA* **97**: 12846–12851.

34. Shah, K, Jacobs, A, Breakefield, XO and Weissleder, R (2004). Molecular imaging of gene therapy for cancer. *Gene Ther* **11**: 1175–1187.
35. Briat, A and Vassaux G (2006). Preclinical applications of imaging for cancer gene therapy. *Expert Rev Mol Med* **8**: 1–19.
36. Ullrich, N, Bordey, A, Gillespie, GY and Sontheimer, H (1998). Expression of voltate-activated chloride currents in acute slices of human gliomas. *Neurosci* **83**: 1161–1173.
37. Deshane, J, Garner, CC and Sontheimer, H (2003). Chlorotoxin inhibits glioma cell invasion via matrix metalloproteinase-2. *J Biol Chem* **278**: 4135–4144.
38. Ernest, NJ, Weaver, AK, Van Duyn, LB and Sontheimer, HW (2005). Relative contribution of chloride channels and transporters to regulatory volume decrease in human glioma cells. *Am J Physiol* **288**: C1451–C1460.
39. Shen, MR, Chou, CY and Ellory, JC (2000). Volume-sensitive KCl cotransport associated with human cervical carcinogenesis. *Pflugers Arch* **440**: 751–760.
40. Riesco-Eizaguirre, G and Santisteban, P (2006). A perspective view of sodium iodide symporter research and its clinical implications. *Eur J Endocrinol* **155**: 495–512.
41. Huang, M, Batra, RK, Kogai, T, Lin, YQ, Hershman, JM, Lichtenstein, A *et al.* (2001). Ectopic expression of the thyroperoxidase gene augments radioiodide uptake and retention mediated by the sodium iodide symporter in non-small cell lung cancer. *Cancer Gene Ther* **8**: 612–618.
42. Furuya, F, Shimura, H, Miyazaki, A, Taki, K, Ohta, K, Haraguchi, K *et al.* (2004). Adenovirus-mediated transfer of thyroid transcription factor-1 induces radioiodide organification and retention in thyroid cancer cells. *Endocrinology* **145**: 5397–5405.
43. Dingli, D, Kemp, BJ, O'Connor, MK, Morris, JC, Russell, SJ and Lowe, VJ (2006). Combined I-124 positron emission tomography/computed tomography imaging of NIS gene expression in animal models of stably transfected and intravenously transfected tumor. *Mol Imaging Biol* **8**: 16–23.
44. Oliveira, R, Christov, C, Guillamo, JS, de Bouard, S, Palfi, S, Venance, L *et al.* (2005). Contribution of gap junctional communication between tumor cells and astroglia to the invasion of the brain parenchyma by human glioblastomas. *BMC Cell Biol* **6**: 7.
45. Zhang, W, DeMattia, JA, Song, H and Couldwell, WT (2003). Communication between malignant glioma cells and vascular endothelial cells through gap junctions. *J Neurosurg* **98**: 846–853.
46. Fechner, H, Wang, X, Pico, AH, Wildner, J, Suckau, L, Pinkert, S *et al.* (2007). A bidirectional Tet-dependent promotor construct regulating the expression of E1A for tight control of oncolytic adenovirus replication. *J Biotechnol* **127**: 560–574.
47. Jimenez, T, Fox, WP, Naus, CC, Galipeau, J and Belliveau, DJ (2006). Connexin over-expression differentially suppresses glioma growth and contributes to the bystander effect following HSV-thymidine kinase gene therapy. *Cell Commun Adhes* **13**: 79–92.
48. Martuza, RL and Eldridge, R (1988). Neurofibromatosis 2 (bilateral acoustic neurofibromatosis). *N Engl J Med* **318**: 684–688.
49. Sena-Esteves, M, Saeki, Y, Camp, SM, Chiocca, EA and Breakefield, XO (1999). Single-step conversion of cells to retrovirus vector producers with herpes simplex virus-Epstein-Barr virus hybrid amplicons. *J Virol* **73**: 10426–10439.
50. García-Añoveros, J, Samad, TA, Zuvela-Jelaska, L, Woolf, CJ and Corey, DP (2001). Transport and localization of the DEG/ENaC ion channel BNaC1alpha to peripheral mechanosensory terminals of dorsal root ganglia neurons. *J Neurosci* **21**: 2678–2686.